Cross section expansion for direct neutron radiative capture

D. Baye
Physique Quantique, CP165/82, Physique Nucléaire Théorique et Physique Mathématique, CP 229, Université Libre de Bruxelles, B 1050 Brussels, Belgium
(Received 5 May 2004; published 7 July 2004)

Cross sections for neutron radiative capture multiplied by the relative velocity can be expressed as a Taylor expansion in powers of the relative energy. The coefficients of this expansion are expressed in the potential model as integrals involving solutions of the radial Schrödinger equation and of its inhomogeneous energy derivatives calculated at zero energy. Similarities and differences with charged-particle capture are emphasized. The $^{12}C(n,\gamma)^{13}C$ capture reaction is treated as an example. The coefficients of the Taylor expansion lead to simple parametrizations of the experimental partial cross sections for neutron capture to each ^{13}C bound state.

DOI: 10.1103/PhysRevC.70.015801 PACS number(s): 25.40.Lw, 28.20.Fc, 24.50.+g, 24.10.Ht

I. INTRODUCTION

In astrophysics, the determination of reaction rates requires accurate values of radiative-capture cross sections down to very low energies [1–3]. Extrapolating a model to those energies and even to zero energy may lead to inaccuracies because the wave functions describing the initial scattering states of the system become very small. This problem can be circumvented by calculating a Taylor expansion near zero energy of a quantity related to the cross section but which does not vanish at zero energy.

This procedure has been applied in Ref. [4] for radiative-capture reactions between charged particles. A Taylor expansion of the astrophysical S factor has been derived in the potential model. The quantities $S(0)$, $S'(0)$, $S''(0)$, … are directly obtained from a calculation of the scattering wave function and of its energy derivatives, at zero energy.

A similar expansion for neutron radiative capture is not available, probably because numerical extrapolations are less difficult in a case without a Coulomb barrier. Such an expansion is, however, useful as it reveals the importance of the different physical ingredients near zero energy. Also it may simplify cross sections parametrizations, increase their accuracy, and allow an optimization of the selection of energies where experiments should be performed. Its derivation is the main purpose of this paper.

A Taylor expansion is shown to exist for σv,

$$\sigma v \propto E^l(1 + s_1E + s_2E^2 + \dots), \tag{1}$$

where $\sigma(E)$ is a partial capture cross section to a given bound state at relative energy E, v is the initial relative velocity, and l is the smallest relevant orbital momentum of the initial scattering state. The coefficients of this Taylor expansion are derived by a simple direct calculation. This expansion is expressed in a notation [5] very close to that employed in the Coulomb case [4] in order to emphasize similarities in the treatment. Nevertheless the low-energy behavior is very different. The natural variable for expansion (1) is the energy E and not its square root $\sqrt{E}$ as rather strangely used in Ref. [1].

The $^{12}C(n,\gamma)^{13}C$ capture reaction has been studied experimentally in detail not only at thermal energy [6,7] but also for neutron energies between 21 and 550 keV [8–10]. The results reveal a strong deviation from a $1/v$ law, which has been discussed by several authors in the potential model [11–13] and in the microscopic cluster model [14]. The present approach allows clarifying the reasons for the deviation from the $1/v$ law. As in a similar study of proton capture by ^{7}Be [15,16], it also provides a better physical understanding of the most relevant quantities at low energies. Expansion (1) can be calculated for each bound state in the case of the $^{12}C(n,\gamma)^{13}C$ capture reaction. The obtained model coefficients s_1 and s_2 are then used together with adjusted spectroscopic factors to determine a simple parametrization of the different experimental partial capture cross sections.

In Sec. II, the formula for the cross section in the potential model is recalled and its low-energy dependence is studied. In Sec. III, the coefficients of the effective-range expansion and of the Taylor expansion (1) are determined. The procedure is illustrated with the $^{12}C(n,\gamma)^{13}C$ reaction in Sec. IV. Concluding remarks are presented in Sec. V.

II. CROSS SECTION NEAR ZERO ENERGY

A nucleus with mass $A_1=A-1$ and charge Z captures a neutron by emitting a photon with wave number k_γ. The energy of the final bound state with respect to the elastic threshold is denoted as E_B. Let I_1 and $I_2=1/2$ be the respective spins of the nucleus and the neutron and I be the total spin. In the potential model, I is both the channel spin of the scattering wave function and the total intrinsic spin of the final nucleus. Let l_i and l_f be the initial and final orbital angular momenta for the relative motions of the neutron-nucleus system and J_i and J_f be the initial and final total angular momenta resulting from the coupling with the total spin I.

The radiative-capture cross section in the potential model is given for example in Ref. [3]. For an electric transition of multipolarity λ, it reads

$$\sigma_{E\lambda}(E) = \alpha(c/v)N_{E\lambda}k_\gamma^{2\lambda+1}[\tilde{I}(E)]^2, \tag{2}$$

where α is the fine structure constant and v is the relative velocity of the particles. In practice, this expression is mul-

tiplied by a spectroscopic factor for each component of the final state and summed over initial or final angular momenta. Since we are dealing here with low-energy dependences, which may vary from one transition to another, these summations are not performed and spectroscopic factors are not introduced for the moment.

In Eq. (2), the normalization factor for $E\lambda$ neutron capture is given by

$$N_{E\lambda} = 8\pi \frac{Z^2}{A^{2\lambda}} \frac{(\lambda+1)(2\lambda+1)}{\lambda(2\lambda+1)!!^2} \times \frac{(2J_i+1)(2J_f+1)(2l_i+1)(2l_f+1)}{2(2I_1+1)} \times \begin{pmatrix} l_f & \lambda & l_i \\ 0 & 0 & 0 \end{pmatrix}^2 \begin{Bmatrix} J_f & l_f & I \\ l_i & J_i & \lambda \end{Bmatrix}^2. \quad (3)$$

The photon wave number k_γ is related to the initial energy E through

$$k_\gamma = (|E_B| + E)/\hbar c. \quad (4)$$

The matrix element $\tilde{I}(E)$ is given by the one-dimensional integral

$$\tilde{I}(E) = \int_0^\infty u_{l_f}(r) r^\lambda \tilde{u}_{l_i}(E,r) dr, \quad (5)$$

where $\tilde{u}_{l_i}(E,r) \equiv \tilde{u}_{l_i I J_i}(E,r)$ and $u_{l_f}(r) \equiv u_{l_f I J_f}(r)$ are, respectively, the initial and final radial wave functions. These wave functions are solutions of the Schrödinger equation

$$H_l u_l = E u_l, \quad (6)$$

with respective energies E and E_B. In Eq. (6), the Hamiltonian reads

$$H_l = -\frac{\hbar^2}{2\mu}\left[\frac{d^2}{dr^2} - \frac{l(l+1)}{r^2}\right] + V(r), \quad (7)$$

where μ is the reduced mass of the system and V is a neutron-nucleus interaction that may depend on l, I, and J. Equations (2) and (5) require a definition of the normalization of $\tilde{u}_{l_i}$ given here by

$$\tilde{u}_l(E,r) \underset{r\to\infty}{\to} r[\cos\ \delta_l(E) j_l(kr) + \sin\ \delta_l(E) n_l(kr)], \quad (8)$$

where j_l and n_l are spherical Bessel functions [17] and δ_l is the phase shift.

When E tends towards zero, the regular function $j_l(kr)$ tends to zero for $l>0$ while the irregular function $n_l(kr)$ tends to infinity [17]. Therefore, rescaled functions are defined [5] as

$$\mathcal{F}_l(E,r) = k^{-l} r j_l(kr) \quad (9)$$

and

$$\mathcal{G}_l(E,r) = k^{l+1} r n_l(kr) \quad (10)$$

for which the same notation is used as for rescaled Coulomb functions in Ref. [4]. The advantage of $\mathcal{F}_l$ and $\mathcal{G}_l$ is that they have a finite limit when $E\to 0$. From the properties of the spherical Bessel functions [17], one deduces their Wronskian at any energy

$$W\{\mathcal{G}_l, \mathcal{F}_l\} = 1, \quad (11)$$

where $W\{g,f\} = g(df/dr) - f(dg/dr)$. In Eqs. (9) and (10), the rescaled Bessel functions directly depend on the energy E. In the following, primes designate derivatives with respect to energy. For example, one has

$$\mathcal{F}_l'(E,r) = \frac{\partial}{\partial E}\mathcal{F}_l(E,r), \quad \mathcal{F}_l''(E,r) = \frac{\partial^2}{\partial E^2}\mathcal{F}_l(E,r) \quad (12)$$

and similar expressions for other functions.

Let me introduce the rescaled partial wave function

$$u_l(E,r) = \tilde{u}_l(E,r)/[k^l \cos\ \delta_l(E)]. \quad (13)$$

As shown hereafter, this normalization ensures that u_l has a finite limit when E tends towards zero [5]. With Eqs. (8)–(10), the asymptotic form of the radial wave function becomes

$$u_l(E,r) \underset{r\to\infty}{\to} \mathcal{F}_l(E,r) + D_l(E)\mathcal{G}_l(E,r) \quad (14)$$

with

$$D_l(E) = k^{-2l-1} \tan\ \delta_l(E). \quad (15)$$

Since its asymptotic form (14) remains finite at $E=0$, $u_l(E,r)$ does not vanish when E tends to zero. Since the phase shift δ_l tends towards zero as k^{2l+1}, function $D_l(E)$ does not vanish either and is given by Eq. (14) as

$$D_l(E) = -\lim_{r\to\infty} W\{\mathcal{F}_l, u_l\} = -\frac{2\mu}{\hbar^2}\int_0^\infty \mathcal{F}_l(E,r) V(r) u_l(E,r) dr. \quad (16)$$

Now an "$\mathcal{S}$ factor" for neutron capture from a given partial wave l is introduced as

$$\mathcal{S}(E) = k^{-2l} v \sigma(E). \quad (17)$$

It generalizes to an arbitrary partial wave the quantity with the same notation introduced in Ref. [1]. From Eqs. (2), (5), (13), and (17), one obtains

$$\mathcal{S}_{E\lambda}(E) = \alpha c N_{E\lambda} k_\gamma^{2\lambda+1} \cos^2\delta_l(E)[I(E)]^2, \quad (18)$$

where

$$I(E) = \int_0^\infty u_{l_f}(r) r^\lambda\ u_{l_i}(E,r) dr. \quad (19)$$

These expressions have a nonvanishing finite limit when E tends towards zero.

In the charged case, the factor $\cos^2\delta_l$ in Eq. (18) can be replaced by unity when a Taylor expansion is performed [4]. Indeed, because of the Coulomb penetration factor, all its derivatives vanish at $E=0$.

III. PROPERTIES AT LOW ENERGY

A. Effective-range expansion

The effective-range expansion [18,19] for an arbitrary partial wave [20] is given by

$$\frac{1}{D_l(E)} = -\frac{1}{a_l} + \frac{1}{2} r_l k^2 - P_l r_l^3 k^4 + O(k^6), \tag{20}$$

where notation (15) is used and a_l, r_l, and P_l are the scattering length, effective range, and shape parameter, respectively.

By performing the Taylor expansion of the left-hand side of Eq. (20), one obtains the scattering length

$$a_l = -D_l(0), \tag{21}$$

the effective range

$$r_l = -\frac{\hbar^2}{\mu a_l^2} D_l'(0), \tag{22}$$

and the shape parameter P_l

$$P_l = \frac{a_l}{4 r_l}\left[1 + \left(\frac{\hbar^2}{\mu}\right)^2 \frac{D_l''(0)}{2 r_l^2 a_l^3}\right]. \tag{23}$$

The low-energy behavior of factor $\cos^2\delta_l$ in Eq. (18) is needed below. For $l>0$, one has

$$\cos^2\,\delta_l = 1 + O(E^{2l+1}), \tag{24}$$

i.e., no contribution up to E^2. On the contrary, for $l=0$, one has

$$\cos^2\,\delta_l = 1 - \frac{2\mu a_0^2}{\hbar^2} E + \left(\frac{2\mu a_0^2}{\hbar^2}\right)^2 \left(1 - \frac{r_0}{a_0}\right) E^2 + O(E^3). \tag{25}$$

This will introduce a difference between the s wave and other waves, which has no equivalent in the charged case.

B. Expansion of $\mathcal{S}(E)$

The Taylor expansion of the $\mathcal{S}$ factor near zero energy can be written as

$$\mathcal{S}(E) \approx \mathcal{S}(0)(1 + s_1 E + s_2 E^2). \tag{26}$$

From Eqs. (18), (19), (24), and (25), one obtains

$$\mathcal{S}(0) = \alpha c N_{\mathrm{E}\lambda} (|E_B|/\hbar c)^{2\lambda+1} [I(0)]^2, \tag{27}$$

with the integral

$$I(0) = \int_0^\infty u_{l_f}(r) r^\lambda\, u_{l_i}^0(r) dr. \tag{28}$$

Here and in the following, the superscript 0 indicates the limiting value for E tending towards zero. The radial wave function $u_l^0(r) \equiv u_l(0,r)$ is a solution of the Schrödinger equation at zero energy,

$$H_l u_l^0 = 0, \tag{29}$$

with the boundary conditions $u_l^0(0)=0$ and

$$u_l^0(r) \underset{r\to\infty}{\to} \mathcal{F}_l^0(r) + D_l(0)\mathcal{G}_l^0(r), \tag{30}$$

where $\mathcal{F}_l^0$ and $\mathcal{G}_l^0$ are the zero-energy limits of $\mathcal{F}_l$ and $\mathcal{G}_l$ (see the Appendix). The function u_l^0 can be normalized by imposing the Wronskian limit

$$W\{\mathcal{G}_l^0, u_l^0\} \underset{r\to\infty}{\to} 1. \tag{31}$$

Using Eqs. (11), (16), and (A1), one obtains the scattering length (21)

$$a_l = \frac{2\mu}{\hbar^2} \frac{1}{(2l+1)!!} \int_0^\infty r^{l+1} V(r) u_l^0(r) dr. \tag{32}$$

The first-order coefficient s_1 in Eq. (26) is obtained by differentiating Eq. (18) with respect to E [4], yielding

$$s_1 = \frac{\mathcal{S}'(0)}{\mathcal{S}(0)} = \frac{2\lambda+1}{|E_B|} + \frac{2I'(0)}{I(0)} - \delta_{l0}\frac{2\mu a_0^2}{\hbar^2}, \tag{33}$$

with the energy derivative of integral (19) given by

$$I'(0) = \int_0^\infty u_{l_f}(r) r^\lambda\, u_{l_i}'^0(r) dr. \tag{34}$$

The energy derivative $u_l'^0$ of the radial wave function at zero energy is a solution of the derivative of the Schrödinger equation (6) at the limit $E\to 0$, i.e.,

$$H_l u_l'^0 = u_l^0. \tag{35}$$

The required solution of this inhomogeneous differential equation verifies $u_l'^0(0)=0$. Its asymptotic form is given by the energy derivative of Eq. (14) at the limit $E\to 0$ as

$$u_l'^0(r) \underset{r\to\infty}{\to} \mathcal{F}_l'^0(r) + D_l(0)\mathcal{G}_l'^0(r) + D_l'(0)\mathcal{G}_l^0(r), \tag{36}$$

where $\mathcal{F}_l'^0(r)$ and $\mathcal{G}_l'^0(r)$ are given by Eqs. (A1) and (A2), respectively. In this expression, $D_l'(0)$ is still unknown.

A solution of Eq. (35) vanishing at the origin may still differ from $u_l'^0$ by an arbitrary amount of solution u_l^0 of the homogeneous Schrödinger equation (29) at zero energy. It can be eliminated by imposing the Wronskian limit

$$W\{\mathcal{G}_l^0, u_l'^0 - \mathcal{F}_l'^0 - D_l(0)\mathcal{G}_l'^0\} \underset{r\to\infty}{\to} 0 \tag{37}$$

obtained from Eqs. (36) and (11) [4]. The coefficient $D_l'(0)$ and the effective range r_l can then be calculated from Eqs. (16) and (22).

The last term in Eq. (33) presents an interesting difference with respect to the corresponding expression in the Coulomb case [Eq. (52) of Ref. [4]]. It occurs only for the s wave and takes its origin from the $\cos^2\,\delta_0$ factor in Eq. (18). It is due to the fact that the δ_0 phase shift vanishes proportionally to k in neutron scattering at low energies.

The second coefficient s_2 in the Taylor expansion (26) reads

$$s_2 = \frac{\mathcal{S}''(0)}{2\mathcal{S}(0)} = \frac{\lambda(2\lambda+1)}{E_B^2} + \frac{2(2\lambda+1)}{|E_B|}\frac{I'(0)}{I(0)} + \frac{I''(0)}{I(0)} + \left[\frac{I'(0)}{I(0)}\right]^2 - \delta_{l0}\frac{2\mu a_0^2}{\hbar^2}\left(s_1 + \frac{2\mu a_0 r_0}{\hbar^2}\right), \quad (38)$$

with the second energy derivative of the integral given by

$$I''(0) = \int_0^\infty u_{l_f}(r) r^\lambda \, u''^0_{l_i}(r) dr. \quad (39)$$

The second derivative u''^0_l can be determined by differentiating Eq. (6) twice with respect to energy and by taking the limit $E \to 0$, i.e.,

$$H_l u''^0_l = 2u'^0_l, \quad (40)$$

with the boundary condition $u''^0_l(0)=0$. Its asymptotic form is fixed by the second energy derivative of Eq. (14),

$$u''^0_l(r) \underset{r\to\infty}{\to} \mathcal{F}''^0_l(r) + D_l(0)\mathcal{G}''^0_l(r) + 2D'_l(0)\mathcal{G}'^0_l(r) + D''_l(0)\mathcal{G}^0_l(r), \quad (41)$$

where $\mathcal{F}''^0_l(r)$ and $\mathcal{G}''^0_l(r)$ are given by Eqs. (A1) and (A2), respectively. Again a solution of the inhomogeneous equation (40) vanishing at the origin may contain an arbitrary amount of u^0_l, which can be eliminated by imposing the condition

$$W\{\mathcal{G}^0_l, u''^0_l - \mathcal{F}''^0_l - D_l(0)\mathcal{G}''^0_l - 2D'_l(0)\mathcal{G}'^0_l\} \underset{r\to\infty}{\to} 0 \quad (42)$$

obtained from Eqs. (41) and (11) [4]. The shape parameter can be obtained from Eqs. (23) and (16). The last term in Eq. (38) for the s wave also takes its origin from the $\cos^2\delta_0$ factor in Eq. (18).

IV. ^{12}C$(n,\gamma)^{13}$C CAPTURE REACTION

The ^{12}C$(n,\gamma)^{13}$C capture reaction is a perfect example illustrating the interest of the present expansion. Indeed, experimental data exist from thermal energy [6,7] up to a neutron energy of 0.55 MeV [8–10] for all ^{13}C bound states. In the following, energies are in MeV and lengths in fm.

In order to derive values of the parameters in expansion (26), I choose a simple Woods-Saxon potential

$$V(r) = -\frac{V_0 + 5.5\boldsymbol{L}\cdot\boldsymbol{S}}{1+\exp[(r-2.86)/0.65]}. \quad (43)$$

Its range and diffuseness are adopted from Refs. [10,13]. The spin-orbit strength of 5.5 MeV is adjusted on the $d3/2$ -$d5/2$ energy difference. The depth V_0 of the central part is adjusted for each bound-state energy. The obtained values are given in Table I.

The corresponding scattering lengths a_{lJ} and effective ranges r_{lJ} obtained with Eqs. (21) and (22), respectively, are also displayed. The s-wave scattering length and effective range are in reasonable agreement with the respective experimental values 6.14 and 3.42 fm [21]. It is interesting to note that the effective range is well fixed by the binding energies and scattering lengths. Indeed, expansion (20) is valid for the imaginary value $k=i\kappa_{lJ}$, where $\kappa_{lJ}=(2\mu|E_{lJ}|/\hbar^2)^{1/2}$, corresponding to a bound state for which $\cot\delta_{lJ}=i$. To the extent that terms beyond k^2 are negligible in the right-hand side of Eq. (20), the effective ranges are approximately given by the generalized Schwinger relation [18,19,22]

$$r'_{lJ} \approx -\frac{2}{\kappa_{lJ}^2}\left[\frac{1}{a_{lJ}} + (-1)^{l+1}\kappa_{lJ}^{2l+1}\right]. \quad (44)$$

TABLE I. Energies E_{lJ} (in MeV), potential depths V_0 (in MeV), scattering lengths a_{lJ} (in fm^{2l+1}), and effective ranges r_{lJ} (in fm^{-2l+1}). The approximate effective ranges r'_{lJ} in the last column are obtained with Eq. (44). The $p3/2$ state in parentheses is forbidden. A potential binding this state at the correct energy is shown in the last row.

lJ	E_{lJ}	V_0	a_{lJ}	r_{lJ}	r'_{lJ}
$s1/2$	−1.86	57.6	6.43	3.56	3.19
$p3/2$	(−9.27)	45.1	8.85	−1.71	−1.83
$p1/2$	−4.96	45.1	22.75	−1.16	−1.34
$d5/2$	−1.10	56.15	159.9	−0.32	−0.25
$d3/2$	+3.3	56.15	−57.2	−0.065	
$p3/2$	−1.28	28.35			

The values r'_{lJ} deduced from Eq. (44) are given in the last column of Table I. They reproduce fairly well the exact values. The experimental scattering length leads to an effective range of 3.02 fm.

The present single-particle model is not able to describe the $p3/2$ bound state. However, in order to study it together with the other bound states, a V_0 value is fitted to the experimental energy for that case too. It is displayed in the last row of Table I. Since it is used for a bound state only, its scattering properties are not necessary.

The coefficients of expansion (26) derived from Eqs. (27), (33), and (38) with the potentials of Table I for $E1$ transitions are displayed in Table II. The zero-energy wave functions are calculated with the Numerov method [23] as explained in Ref. [4]. Coefficient s_1 induces a deviation from a v^{2l_i-1} law. One observes that it is often negative in Table II. Only in the s-wave capture to the $3/2^-$ state is the $1/v$ law valid in the present model.

Experimental data can be fitted with expansion (26) to determine parameters $\mathcal{S}(0)$, s_1, and s_2. This approach is feasible but hindered by large error bars on the data. Therefore I make the following assumption: the coefficients s_1 and s_2 are only weakly model dependent. In the following, their unchanged model values will be used in fits of the data while the $\mathcal{S}(0)$ values will be adjusted to the data. The resulting correcting factors $\mathcal{S}_{\rm expt}(0)/\mathcal{S}(0)$ are given in the last column of Table II.

The capture to the $1/2^-$ ground state is presented in Fig. 1. The parameter $\mathcal{S}(0)$ is reduced by a factor 0.88 (see Table II) in order to fit the accurate experimental value 2.38 ± 0.05 mb at thermal energy [6,7], which is indistinguishable from $E=0$ with the linear energy scale in Fig. 1.

TABLE II. Coefficients $\mathcal{S}(0)$ (in $\mathrm{fm}^{2l+3}\mathrm{s}^{-1}$), s_1 (in MeV^{-1}), and s_2 (in MeV^{-2}) of expansion (26) for different transitions. The numbers in the last column are fitted to experiment as explained in the text.

$l_f J_f$	$l_i J_i$	$\mathcal{S}(0)$	s_1	s_2	$\mathcal{S}_{\mathrm{expt}}(0)/\mathcal{S}(0)$
$p1/2$	$s1/2$	5.90×10^{17}	−1.10	0.70	0.88
	$d3/2$	3.91×10^{21}	0.13	0.17	0.88
$s1/2$	$p3/2$	1.09×10^{21}	−0.77	0.52	0.95
	$p1/2$	4.74×10^{20}	−1.02	0.97	0.95
$p3/2$	$s1/2$	1.67×10^{18}	−0.012	0.026	0.15
	$d5/2$	4.72×10^{21}	−0.99	0.55	1.0
	$d3/2$	7.83×10^{20}	−0.60	0.48	1.0
$d5/2$	$p3/2$	1.29×10^{20}	−0.27	0.12	0.39

The resulting s wave approximation involving s_1 and s_2 is displayed as a dashed line. In order to check the validity of the Taylor expansion, it is compared with the exact result obtained from Eq. (2) also multiplied by the correcting factor $\mathcal{S}_{\mathrm{expt}}(0)/\mathcal{S}(0)$, represented as a dotted line. The second-degree polynomial (26) is quite accurate. However, the resulting curve is far from the data. The d-wave term $k^4\mathcal{S}_{d3/2\to p1/2}(E)$ must be added. It would need be multiplied by a factor 0.64 in order to fit the data point at $E=0.508$ MeV ($E_n=0.55$ MeV). However, I use instead the same factor as for the other partial wave. The total $\mathcal{S}$ factor

$$\mathcal{S}_{1/2^-}(E) = 0.88[\mathcal{S}_{s1/2\to p1/2}(E) + k^4\mathcal{S}_{d3/2\to p1/2}(E)] \quad (45)$$

is represented as a full line in Fig. 1. It agrees with the data over the whole energy range. The exact calculation is almost identical.

The correcting factor 0.88 can be interpreted as a spectroscopic factor for the ground state [24]. This value is consistent with the experimental result 0.84 ± 0.04 of Ref. [25]. The same spectroscopic factor is thus employed in Eq. (45) for the transition from the d state. Unless the $s_2=0.70$ value for the s wave is very incorrect, the calculation indicates that the cross section at 0.509 MeV should be close to the upper limit of the error bar.

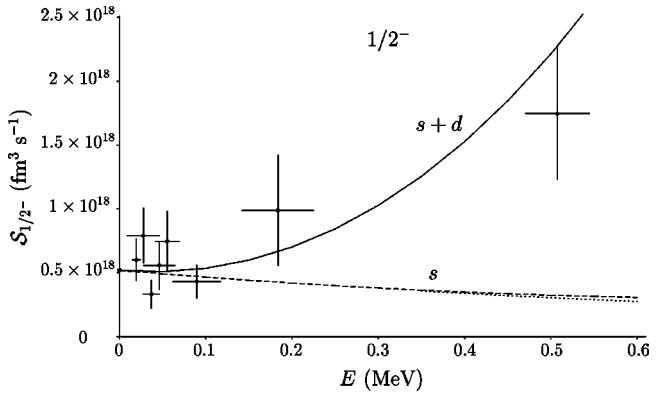

FIG. 1. $\mathcal{S}$ factor for radiative capture to the $1/2^-$ ground state of ^{13}C: parametrization (26) for s-wave capture (dashed line), potential-model calculation for s-wave capture (dotted line), and parametrization (45) for s and d wave capture (full line). Experimental data are from Refs. [6–10].

The factor $\mathcal{S}_{1/2^+}$ for the capture to the $1/2^+$ excited state is presented in Fig. 2. Both initial components $p1/2$ and $p3/2$ are summed. The parameter $\mathcal{S}(0)$ is reduced by a factor 0.95 in order to fit the experimental point at 0.509 MeV. The resulting s wave approximation involving s_1 and s_2 is displayed as a full line. It closely follows the trends of the data, indicating that s_1 and s_2 are reasonable. The exact result obtained from Eq. (2), also multiplied by the correcting factor 0.95, is represented as a dotted line and is not very different from its approximation. The second-degree polynomial (26) is thus quite accurate. The obtained spectroscopic factor is in good agreement with a previous determination [26], although Eq. (32) does not seem to support a derivation of the spectroscopic factor based on the scattering length.

Interestingly, the present parametrization cannot explain the thermal cross section 5.6 ± 0.4 μb to the $1/2^+$ state [6,7]. It underestimates this value by several orders of magnitude. This thermal cross section is thus clear evidence for $M1$ capture. Unfortunately, the $M1$ capture cross section vanishes exactly in the potential model because the initial and final wave functions in the integral $I(E)$ (without the r^λ factor) are orthogonal as they both belong to the s wave. This $M1$ capture represents an interesting challenge for more elaborate models. Strikingly it would also vanish in a single-channel microscopic model [27].

The procedure for the $3/2^-$ excited state is very close to that for the ground state (see Fig. 3) but the use of the po-

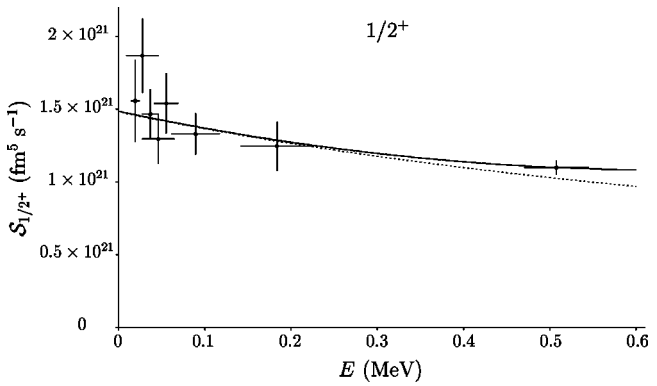

FIG. 2. $\mathcal{S}$ factor for radiative capture to the $1/2^+$ state of ^{13}C: parametrization (26) for $p1/2$ and $p3/2$ wave capture (full line) and potential-model calculation (dotted line). Experimental data are from Refs. [8–10].

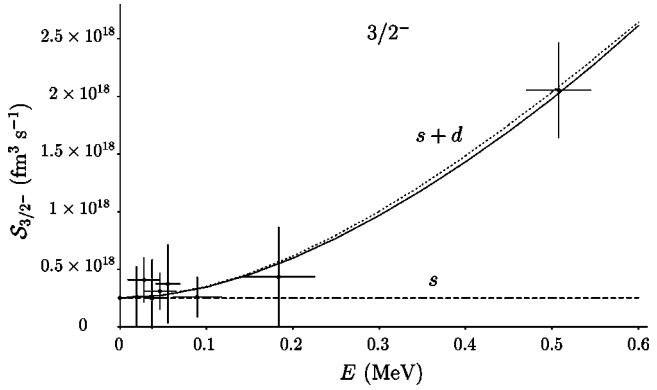

FIG. 3. $\mathcal{S}$ factor for radiative capture to the $3/2^-$ state of ^{13}C: parametrization (26) for *s*-wave capture (dashed line), sum of parametrizations for *s* and *d* wave capture (full line), and potential-model calculation for *s* and *d* wave capture (dotted line). Experimental data are from Refs. [6–10].

tential model is here rather artificial. The initial *s* component fitted to the experimental thermal cross section 1.14 ± 0.02 mb [6,7] is represented as a dashed line. The correcting factor 0.15 is compatible with spectroscopic factors for that state [28]. The initial $d5/2$ and $d3/2$ components are added to fit the data point at 0.509 MeV. Here no multiplicative factor is needed. The factor $\mathcal{S}_{3/2^-}$ for the capture to the $3/2^-$ excited state is then obtained with a formula similar to Eq. (45) but with different factors for both terms. An exact calculation with the same multiplicative factors (dotted line) is very close to the present approximation. The use of such different correcting factors cannot easily be explained but may reflect the fact that the coefficient s_2 of the *s* wave should be much larger.

Finally the factor $\mathcal{S}_{5/2^+}$ for capture to the $5/2^+$ excited state is presented in Fig. 4. The correcting factor fitted at 0.509 MeV is 0.39, a value rather different from spectroscopic factors for that state [28]. The exact calculation shows no difference. Here one can suspect that the theoretical values of s_1 and s_2 are inaccurate. The data seem to indicate that the slope s_1 should be negative, which would lead to a larger value of $\mathcal{S}_{\rm expt}(0)/\mathcal{S}(0)$. However, the error bars are too large to lead to definite conclusions.

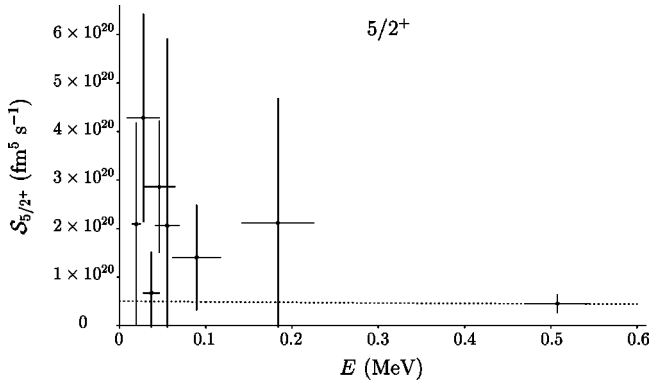

FIG. 4. $\mathcal{S}$ factor for radiative capture to the $5/2^+$ state of ^{13}C: parametrization (26) for $p3/2$-wave capture (dotted line). Experimental data are from Refs. [8–10].

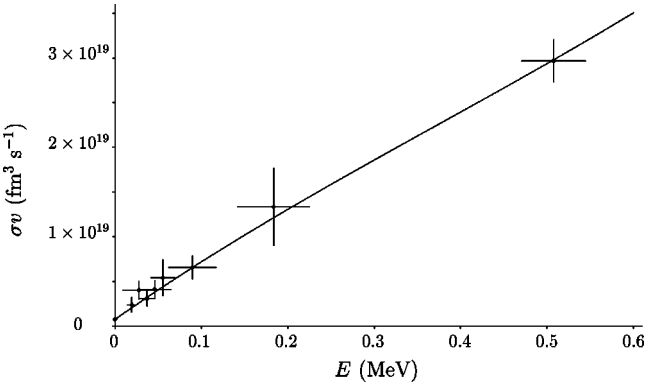

FIG. 5. Total σv product for ^{12}C$(n,\gamma)^{13}$C radiative capture: parametrization (47) (full line). Experimental data are from Refs. [6,8–10].

By summing the capture contributions to the different bound states,

$$\sigma v \approx \mathcal{S}_{1/2^-}(E) + k^2\mathcal{S}_{1/2^+}(E) + \mathcal{S}_{3/2^-}(E) + k^2\mathcal{S}_{5/2^+}(E), \quad (46)$$

one obtains the parametrization

$$\sigma v \approx 7.70\times10^{17}(1 + 88.1E - 50.0E^2 + 44.7E^3)\text{fm}^3\ \text{s}^{-1}. \quad (47)$$

This expression is limited at order 3 for simplicity. It is compared with experimental data in Fig. 5. The fact that the $1/v$ law is not valid here [8,9] is obvious in this figure. As already noted in Refs. [11–14], the large coefficient of the *E* term in Eq. (47) is mostly due to the importance of *p*-wave capture to the $1/2^+$ state.

By averaging expression (47) with a Maxwellian distribution [1,2], one obtains the reaction rate

$$N_A\langle\sigma v\rangle \approx 463(1 + 11.4T_9 - 1.39T_9^2 + 0.37T_9^3)\text{cm}^3\ \text{mol}^{-1}\ \text{s}^{-1}. \quad (48)$$

This rate slightly oscillates around the rate proposed in Ref. [10] with deviations reaching +4% near $T_9=0.2$ and −7% near $T_9=2.5$.

V. CONCLUSIONS

The coefficients of the Taylor expansion of $\mathcal{S}(E) = k^{-2l}v\sigma(E)$ are directly calculated at zero energy. The first terms of this expansion are obtained by solving the Schrödinger equation and its energy derivatives at $E=0$. The results are accurate and can be used to correctly extrapolate standard calculations performed at positive energies.

The method is applied here to the simple potential model but the main ingredients of its algorithm, i.e., the properties of wave functions at zero energy, can straightforwardly be extended to more elaborate models such as microscopic models.

A parametrization with second-order polynomials is valid over an energy range covering the domain of astrophysical interest. With only three coefficients in the parametrization, experimental data at three energies, e.g., thermal energy and

two other energies, may be sufficient to adjust the coefficients. If *p*-wave capture is important, three energies beyond thermal are needed. Alternatively, this type of parametrization can be used for an all-theoretical prediction of the cross sections. With a potential reproducing the different bound-state energies, the coefficients $\mathcal{S}(0)$, s_1, and s_2 are easily obtained. A reliable parametrization should then be obtained with some information on spectroscopic factors.

In the treatment of the $^{12}\mathrm{C}(n,\gamma)^{13}\mathrm{C}$ capture reaction, I have adopted an intermediate strategy. The potential model provides the shape coefficients s_1 and s_2. The remaining normalization coefficients are fitted to experiment at an energy where accurate data exist. This approach provides an excellent parametrization of all data as well as some values of spectroscopic factors. The cross sections show a strong deviation from the $1/v$ law as noticed and explained in several previous works. The essential part of the deviation comes from the *p*-wave capture to the $1/2^+$ bound state. Deviations due at least to coefficients s_1 should occur in most direct neutron capture reactions.

ACKNOWLEDGMENTS

This text presents research results of the Belgian program P5/07 on interuniversity attraction poles initiated by the Belgian-state Federal Services for Scientific, Technical and Cultural Affairs.

APPENDIX

At low energies, functions $\mathcal{F}_l$ and $\mathcal{G}_l$ are given by the Taylor expansions [17,5]

$$\begin{aligned}\mathcal{F}_l(E,r) &= \mathcal{F}_l^0(r) + E\mathcal{F}_l'^0(r) + \frac{1}{2}E^2\mathcal{F}_l''^0(r) + O(E^3)\\ &= \frac{r^{l+1}}{(2l+1)!!}\left[1 - \left(\frac{\mu E}{\hbar^2}\right)\frac{r^2}{(2l+3)} + \left(\frac{\mu E}{\hbar^2}\right)^2\frac{r^4}{2(2l+3)(2l+5)}\right] + O(E^3) \qquad \text{(A1)}\end{aligned}$$

and

$$\begin{aligned}\mathcal{G}_l(E,r) &= \mathcal{G}_l^0(r) + E\mathcal{G}_l'^0(r) + \frac{1}{2}E^2\mathcal{G}_l''^0(r) + O(E^3)\\ &= (2l-1)!!\, r^{-l}\left[1 + \left(\frac{\mu E}{\hbar^2}\right)\frac{r^2}{(2l-1)} + \left(\frac{\mu E}{\hbar^2}\right)^2\frac{r^4}{2(2l-1)(2l-3)}\right] + O(E^3). \qquad \text{(A2)}\end{aligned}$$

[1] W. A. Fowler, G. R. Caughlan, and B. A. Zimmerman, Annu. Rev. Astron. Astrophys. **5**, 525 (1967).

[2] C. E. Rolfs and W. S. Rodney, *Cauldrons in the Cosmos* (University of Chicago, Chicago, 1988).

[3] C. Angulo, M. Arnould, M. Rayet, P. Descouvemont, D. Baye, C. Leclercq-Willain, A. Coc, S. Barhoumi, P. Aguer, C. Rolfs, R. Kunz, J. W. Hammer, A. Mayer, T. Paradellis, S. Kossionides, C. Chronidou, K. Spyrou, S. Degl'Innocenti, G. Fiorentini, B. Ricci, S. Zavatarelli, C. Providencia, H. Wolters, J. Soares, C. Grama, J. Rahighi, A. Shotter, and M. Lamehi Rachti, Nucl. Phys. **A656**, 3 (1999).

[4] D. Baye and E. Brainis, Phys. Rev. C **61**, 025801 (2000).

[5] D. Baye, M. Hesse, and R. Kamouni, Phys. Rev. C **63**, 014605 (2001).

[6] E. T. Jurney, P. J. Bendt, and J. C. Browne, Phys. Rev. C **25**, 2810 (1982).

[7] S. F. Mughabghab, M. A. Lone, and B. C. Robertson, Phys. Rev. C **26**, 2698 (1982).

[8] Y. Nagai, M. Igashira, K. Takeda, N. Mukai, S. Motoyama, F. Uesawa, H. Kitazawa, and T. Fukuda, Astrophys. J. **372**, 683 (1991).

[9] T. Ohsaki, Y. Nagai, M. Igashira, T. Shima, K. Takeda, S. Seino, and T. Irie, Astrophys. J. **422**, 912 (1994).

[10] T. Kikuchi, Y. Nagai, T. S. Suzuki, T. Shima, T. Kii, M. Igashira, A. Mengoni, and T. Otsuka, Phys. Rev. C **57**, 2724 (1998).

[11] Y.-K. Ho, H. Kitazawa, and M. Igashira, Phys. Rev. C **44**, 1148 (1991).

[12] A. Mengoni, T. Otsuka, and M. Ishihara, Phys. Rev. C **52**, R2334 (1995).

[13] C. J. Lin, H. Q. Zhang, Z. H. Liu, W. Y. Wu, F. Wang, and M. Ruan, Phys. Rev. C **68**, 047601 (2003).

[14] M. Dufour and P. Descouvemont, Phys. Rev. C **56**, 1831 (1997).

[15] D. Baye, Phys. Rev. C **62**, 065803 (2000).

[16] C. Angulo, M. Azzouz, P. Descouvemont, D. Baye, M. Cogneau, M. Couder, T. Davinson, A. Di Pietro, P. Figuera, M. Gaelens, P. Leleux, M. Loiselet, F. de Oliveira Santos, R. G. Pizzone, G. Ryckewaert, N. de Séréville, G. Tabacaru, and F. Vanderbist, Nucl. Phys. **A716**, 211 (2003).

[17] M. Abramowitz and I. A. Stegun, *Handbook of Mathematical Functions* (Dover, New York, 1970).

[18] H. A. Bethe, Phys. Rev. **76**, 38 (1949).

[19] M. A. Preston and R. K. Bhaduri, *Structure of the Nucleus* (Addison-Wesley, Reading, MA 1975).

[20] T. Teichmann, Phys. Rev. **83**, 141 (1951).

[21] F. Ajzenberg-Selove, Nucl. Phys. **A449**, 1 (1986).

[22] S. Flügge, *Practical Quantum Mechanics I* (Springer, Berlin, 1971), p. 238.

[23] J. Raynal, *Computing as a Language of Physics*, Trieste, 1971 (IAEA, Vienna, 1972) p. 281.

[24] H. Beer, C. Coceva, P. V. Sedyshev, Y. P. Popov, H. Herndl, R. Hofinger, P. Mohr, and H. Oberhummer, Phys. Rev. C **54**, 2014 (1996).

[25] H. P. Gubler, G. R. Plattner, I. Sick, A. Traber, and W. Weiss, Nucl. Phys. **A284**, 114 (1977).

[26] P. Mohr, H. Herndl, and H. Oberhummer, Phys. Rev. C **55**, 1591 (1997).

[27] D. Baye and P. Descouvemont, Nucl. Phys. **A407**, 77 (1983).

[28] F. C. Barker and N. Ferdous, Aust. J. Phys. **33**, 691 (1980).